

Interplay of breakup and fusion in near-barrier collisions of weakly-bound nuclides

E. C. Simpson^{1,*}, K. J. Cook¹, L. T. Bezzina¹, I. P. Carter¹, M. Dasgupta¹, and D. J. Hinde¹

¹Department of Nuclear Physics and Accelerator Applications, Research School of Physics, Australian National University, Canberra ACT 2601 Australia

Abstract.

Light, weakly-bound nuclides such as ${}^6,7\text{Li}$ and ${}^9\text{Be}$ exhibit a diverse range of near-barrier reaction phenomena. Complete fusion is found to be suppressed by up to 35% with respect to barrier-passing model calculations. Their weak binding leads to significant breakup through excitation of the continuum, but also through production of weakly-bound or unbound neighbouring nuclides via nucleon transfer. Such systems also exhibit large yields of *incomplete* fusion, which is correlated empirically with cluster breakup thresholds for these stable nuclides.

Disentangling these reaction phenomena and their complex interplay is one of the most interesting challenges in near-barrier reaction dynamics. Here we briefly review our recent progress in understanding the interplay between breakup and fusion. These results strongly suggest that the dominant mechanism leading to incomplete fusion and the suppression of complete fusion is direct capture of the projectile cluster constituents by the target nucleus, rather than requiring projectile breakup prior to fusion.

1 Introduction

Light, weakly-bound stable nuclides show a wide range of near-barrier reaction phenomena. Their weak binding leads to breakup through excitation of the continuum, but also through production of weakly-bound or unbound neighbouring nuclides via nucleon transfer. Complete fusion, experimentally defined as capture of the complete charge of the projectile by the target nucleus, is found to be suppressed by up to 35% with respect to barrier-passing models or reactions of more well-bound nuclei. Furthermore, *partial* charge capture (termed incomplete fusion) is also observed, typically with high probability. Due to the weak binding of the projectile, breakup of the projectile into two charged clusters is also likely. For a given projectile, the suppression of complete fusion, the fraction of incomplete fusion, and the probability of breakup are empirically found to be correlated with the lowest cluster breakup threshold.

Disentangling these reaction phenomena and the various mechanisms at play is a significant challenge in near-barrier reaction dynamics. Specifically, what are the reaction processes that lead to breakup and incomplete fusion, and how and why are they related? Here we briefly review studies of incomplete fusion and near-barrier breakup, and recent progress in understanding the interplay between breakup and fusion. Our recent results for ${}^{7,8}\text{Li}+{}^{209}\text{Bi}$ strongly suggest that the dominant mechanism leading to incomplete fusion and the suppression of complete fusion is direct capture of the cluster constituents by the target.

*e-mail: edward.simpson@anu.edu.au

2 Fusion and breakup in near-barrier collisions

2.1 Suppression of complete fusion

The first strong evidence for the suppression of complete fusion came from high precision measurements for the ${}^9\text{Be}+{}^{208}\text{Pb}$ reaction [1]. Made in part to establish a stable nucleus reference to aid in understanding the fusion of the neutron halo nucleus ${}^{11}\text{Be}$ [2], the measurements for ${}^9\text{Be}$ revealed something puzzling: the measured complete fusion cross section was suppressed by a factor 0.68 ± 0.07 with respect to coupled channels fusion calculations. These included couplings to excited states of ${}^9\text{Be}$ and ${}^{208}\text{Pb}$, but did not include breakup effects. At above-barrier energies, this scaling factor was found to be independent of energy. A large yield of incomplete fusion was observed. The suppression was postulated to be due to breakup of ${}^9\text{Be}$ prior to reaching the fusion barrier, such that only one of the two constituent α -particles was captured by the target. This mechanism could therefore explain both the complete fusion suppression and large incomplete fusion yield. This work was followed by subsequent studies of ${}^{6,7}\text{Li}+{}^{209}\text{Bi}$ [3, 4], which found a similar suppression of complete fusion, by factors ~ 0.65 and ~ 0.74 respectively. The large yield of polonium ($Z = 84$) and astatine ($Z = 85$) compared to the complete fusion cross section had been noted in earlier work [5], which used the same α -decay spectroscopy technique.

Numerous studies identified significant suppression of complete fusion for a variety of light projectiles: ${}^6\text{Li}+{}^{208}\text{Pb}$ [6]; ${}^9\text{Be}+{}^{144}\text{Sm}$ [7]; ${}^{10,11}\text{B}+{}^{159}\text{Tb}$ [8];

${}^8\text{Li}+{}^{208}\text{Pb}$ [9]; ${}^{10,11}\text{B}+{}^{209}\text{Bi}$ [10]; ${}^{10,11}\text{Be}+{}^{209}\text{Bi}$ [2, 11, 12]; ${}^9\text{Be}+{}^{181}\text{Ta}$ [13]. In most of these cases, the degree of suppression was quantified with respect to barrier passing models or coupled channels calculations. It was noted that the degree of fusion suppression was correlated with the α -particle breakup threshold or, more generally, the lowest charged-cluster breakup threshold [8, 10]. Breakup of the clustered projectile nucleus prior to reaching the point of capture therefore appeared the likely mechanism behind both the suppression of complete fusion and large incomplete fusion yields.

2.2 Breakup timescales

The importance of breakup timescales to the possibility of breakup suppressing fusion was recognised in Ref. [14], where α -particles emerging from ${}^9\text{Be}$ interactions with ${}^{208}\text{Pb}$ were measured. A key point here is that for breakup to influence fusion, it must happen *before* the projectile reaches the barrier radius with respect to the target. Breakup couplings to long-lived states ought to act like any other inelastic coupling and enhance fusion rather than suppress it [15].

To study breakup at above-barrier energies is problematic, since in many cases, one of the fragments will be absorbed, as shown by the large cross-sections for incomplete fusion. This would then give incomplete experimental information, and interpretation would pre-suppose an understanding of the mechanisms that were being investigated. Instead, experimental investigations were initiated [14] at below-barrier beam energies, where absorption of the charged breakup fragments should be minimal. By studying the energy distributions of singles α -particles, Hinde *et al.* were able to approximately separate the long-lived (10^{-16}s) breakup via the ${}^8\text{Be}$ ground state from more rapid breakup [14]. The latter will occur at much smaller separation distances from the target nucleus than the ${}^8\text{Be}$ ground state decay, and was found to have sufficient probability to qualitatively explain the suppression of complete fusion. The process of prompt breakup followed by capture of one cluster as a mechanism for incomplete fusion then became a major focus of inquiry.

2.3 Classical trajectory models

In parallel with these successful early sub-barrier breakup measurements, a key question was how to quantitatively relate sub-barrier measurements of breakup cross-sections and probabilities to the above-barrier complete fusion and incomplete fusion cross sections, to allow prediction of these quantities. To model the process of breakup followed by capture, classical trajectory models were developed. The classical trajectory Monte Carlo model of Ref. [16] treated ${}^6\text{Li}$ as a two-body ($\alpha + d$) projectile interacting with a third body (the target). The two fragments of the projectile are initially confined within their mutual potential with an appropriate binding energy. The Newtonian trajectories of the particles are then followed, and if either cluster comes within a given distance with respect to the target it is deemed to have fused. The calculations gave a

good description of the complete fusion and total incomplete fusion cross sections.

Later work [17] followed a slightly different semi-empirical approach, with the aim of mapping from experimental sub-barrier breakup probabilities to above-barrier complete and incomplete fusion cross-sections. Here the position of breakup of the projectile is treated stochastically, with the probability of this occurring parameterised by an empirical exponential *breakup function* $\exp(-\gamma R)$ depending on the separation of the projectile and target R . At the point of breakup, two charged fragments are spawned and their trajectories followed. By simulating many events, cross sections for complete and incomplete fusion can be estimated. The breakup function could be chosen to obtain reasonable agreement with sub-barrier breakup data for ${}^9\text{Be}+{}^{208}\text{Pb}$. However, the slope γ of the deduced breakup function was significantly steeper than that suggested by Continuum Discretised Coupled Channels (CDCC) calculations of breakup, hinting that other reactions mechanisms were important in triggering breakup.

2.4 Reaction mechanisms for prompt breakup

Following this development, further experimental work was undertaken to investigate and understand the processes triggering breakup at a more microscopic level, including both the reaction mechanisms at play and the relevant timescales [18–20]. Charged-particle coincidences were measured at sub-barrier energies (where capture of breakup fragments should be negligible) for reactions of ${}^9\text{Be}$ and ${}^{6,7}\text{Li}$ with various targets from ${}^{144}\text{Sm}$ to ${}^{209}\text{Bi}$. A multitude of different breakup modes were identified: direct breakup for all three cases, but also neutron stripping for ${}^9\text{Be}$, one and two neutron stripping and proton pickup for ${}^7\text{Li}$, and neutron stripping and deuteron pickup for ${}^6\text{Li}$. By considering the relative energy of the coincident emergent fragments narrow resonances could be identified, and prompt and delayed breakup distinguished quantitatively for the first time. Only the prompt breakup would have the capacity to suppress fusion, a significant fraction of which came from transfer-induced breakup. This fraction, often more than half of prompt breakup, tended to increase with beam energy because the transfer probabilities increase faster than electromagnetic excitation as the distance of closest approach reduces.

The question then becomes: how prompt does the breakup have to be to influence fusion, and how can we determine the degree of promptness? If the breakup proceeds via a narrow resonance it occurs asymptotically — that is, when the light nucleus has retreated far from the target — and the relative energy of the two clusters matches that of the resonance. If the breakup were to occur instantaneously, when the projectile is close to the target nucleus, the strong interaction between both the charged breakup fragments and the target nucleus becomes the most important factor in determining the final energies and angles of the fragments. In this case, the relative energy of the α particles is no longer strongly related to the excitation energy in the continuum state from which they originated, unlike in the case of a long-lived resonance. However,

the breakup timescales of a resonance are related to its width Γ , and even wide resonances are unlikely to break up instantaneously. In between the extremes of instantaneous and asymptotic breakup, we have a spectrum of outcomes, where the final relative energy of the clusters switches from being determined by the interactions with the target, to being determined by the properties of the resonance.

Take the example of breakup of ${}^7\text{Li}$ by proton pickup, which forms unbound ${}^8\text{Be}$. ${}^8\text{Be}$ has both a narrow, long-lived 0^+ ground state resonance and a wide, short-lived 2^+ resonance. The long-lived ground state breaks up far from the target and appears as a narrow peak in the relative energy distribution of the two emerging α particles [18–20]. The breakup via the short-lived 2^+ resonance is less clear when considering the relative energy. The ${}^8\text{Be}$ disintegrates promptly and the two resultant α -particles interact strongly with the target nucleus, distorting their relative energy and, more broadly, their energy and angle correlations. However, the degree of this distortion is sensitive to the strength of the interaction with the target and therefore how close the ${}^8\text{Be}$ is to the target when it disintegrates. This question was addressed in Ref.[21], which demonstrated a clear sensitivity of the two breakup fragment kinetic energy and angle correlations to the proximity of the target nucleus at the time of breakup. In the case of the transfer reaction ${}^7\text{Li} \rightarrow {}^8\text{Be}$ in interactions with a ${}^{58}\text{Ni}$ target, it was apparent that the disintegration occurred predominantly while the ${}^8\text{Be}$ was receding from the target nucleus after passing the distance of closest approach. Even though the 2^+ resonance is short-lived, the delay induced in its disintegration is long enough to have a significant impact on the suppression of complete fusion. Given the large width of the 2^+ state (width $\Gamma \approx 1.5$ MeV), it seemed clear that very few resonances would disintegrate fast enough to influence fusion. Similar arguments hold for essentially all transfer-induced breakup for ${}^{6,7}\text{Li}$ and ${}^9\text{Be}$.

Direct breakup of ${}^6\text{Li}$ and ${}^7\text{Li}$ was also studied in a similar fashion and both prompt and asymptotic breakup observed [22]. However, it is harder to attribute the prompt breakup to specific resonances — a significant fraction may come from non-resonant continuum states, and the degree to which the breakup of such states is delayed is unclear.

Further developments were made to classical dynamical models to incorporate the effect of delayed breakup via resonances [21–23]. This addition allowed these classical models to give a good description of no-capture breakup observables. However, there is greater uncertainty regarding their ability to predict incomplete fusion. First and foremost, the calculations use a prescribed breakup function (i.e. the probability of the reaction triggering breakup as a function of distance) which must be taken from comprehensive sub-barrier measurements of no-capture breakup. This dictates the overall breakup yield and the broad likelihood of incomplete fusion.

The classical nature of the model forces us to prescribe further aspects of the dynamics. For example, at the point of a reaction occurring, we cannot simultaneously con-

serve linear momentum, angular momentum and the position of the reactants. Classically forbidden regions pose a further issue. Negative Q -value reactions may be prevented from occurring near the turning point of a classical trajectory — do they then only occur at larger distances, despite the breakup functions suggesting they should occur at shorter distances? These (and other) uncertainties prevent classical dynamical models being genuinely predictive for incomplete fusion cross sections. We thus turn to experiment to provide more concrete guidance on the mechanisms leading to incomplete fusion.

3 Unaccompanied α -particles and the mechanisms leading to incomplete fusion

3.1 ${}^8\text{Li}+{}^{209}\text{Bi}$

We first discuss measurements made of the breakup of ${}^8\text{Li}$ in collisions with ${}^{209}\text{Bi}$ [24]. Previous measurements had suggested a significant suppression of complete fusion comparable to the stable lithium isotopes [9], despite ${}^8\text{Li}$ having a much higher charged-cluster breakup threshold. In the present experiment, the 14UD Tandem Accelerator at the Heavy Ion Accelerator Facility delivered a pulsed beam of ${}^7\text{Li}$ (pulse separation 107 ns, pulse width 1 ns) to a ${}^9\text{Be}$ primary reaction target, producing ${}^8\text{Li}$ via neutron pickup. The secondary ${}^8\text{Li}$ beam had an energy range $E_{c.m.} = 36.8 - 39.4$ MeV (resulting from the thickness of the primary target) which is ~ 1.25 times the fusion barrier energy with the secondary ${}^{209}\text{Bi}$ target. The ${}^8\text{Li}$ was separated from the ${}^7\text{Li}$ primary beam using the SOLEROO solenoidal separator [18, 25] and delivered to the ${}^{209}\text{Bi}$ secondary reaction target. Four large area double-sided silicon strip detectors (Micron Semiconductor MMM design) of the ANU Breakup Array for Light Nuclei (BALiN) were arranged as two telescopes to measure the angle, energy loss and kinetic energy of the two breakup fragments. Particle identification in Z and A was made using the $\Delta E - E$ and time of flight information.

Multiple charged-cluster breakup modes were identified including $\alpha + t$, $\alpha + d$, $\alpha + \alpha$ and $\alpha + p$. Breakup cross-sections were determined through a sophisticated simulation including the reaction dynamics and the detector geometry. This was a key element enabling quantitative conclusions to be reached. When all the cross-sections were compared, the summed yield of α particles from *coincidence* events contributed only 19% of the total observed α yield, with the remaining 81% of α -particles being *unaccompanied* by another light charged fragment. The unobserved fragment must have been captured by the target nucleus.

Since much of the observed breakup into charged fragments is mediated by long-lived resonances, and the cross sections are small compared to the total α -particle cross section, it was concluded that breakup into charged fragments before reaching the capture barrier cannot explain either the observed large total α -particle yield or the previously observed suppression of complete fusion [9].

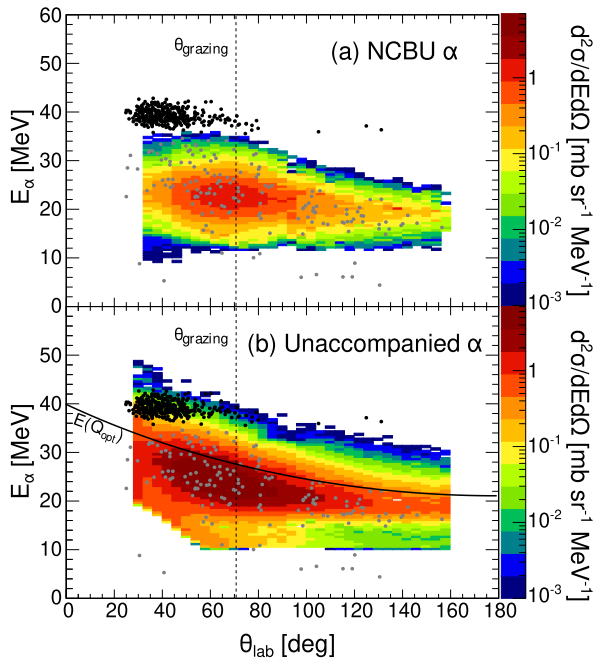


Figure 1. Energy and angle correlation for α -particles measured in reactions of ${}^7\text{Li}+{}^{209}\text{Bi}$. Panel (a) shows α -particles from no-capture breakup that were identified in coincidence with another beam-like fragment. Panel (b) shows α particles that were not accompanied by another projectile-like fragment. The black and grey points show events that were measured in coincidence with the α -decay of ${}^{212}\text{Po}$. See text for further discussion. Adapted from Ref. [26].

3.2 ${}^7\text{Li}+{}^{209}\text{Bi}$

This prompted further investigation. To obtain high statistics, instead of the low yield radioactive ${}^8\text{Li}$ beam, a beam of stable ${}^7\text{Li}$ was used. The aim was to identify and characterise these unaccompanied α -particles and discern their origin [26]. A pulsed ${}^7\text{Li}$ beam (pulse separation 535 ns) interacted with a ${}^{209}\text{Bi}$ target, and BALiN was again used to detect and identify emerging charged clusters. Subtracting the cross sections for no-capture breakup α -particles from the inclusive α -particle spectra allowed cross sections and spectra of the unaccompanied α -particles to be determined.

Figure 1(a) shows the correlation between energy and angle for α -particles which were in coincidence with another charged fragment (i.e. no-capture breakup). The corresponding spectrum of α -particles that were unaccompanied (corresponding to capture of the complementary beam particle fragment, and thus incomplete fusion events) is shown in Figure 1(b). The correlation differs significantly, with the unaccompanied α -particles showing a stronger correlation between energy and angle, peaking at somewhat more forward angles, and extending to significantly higher energies. Assuming a triton transfer, the expected correlation between energy and angle for the optimal Q-value for transfer is shown by the black line, which matches the general trend of the data very well.

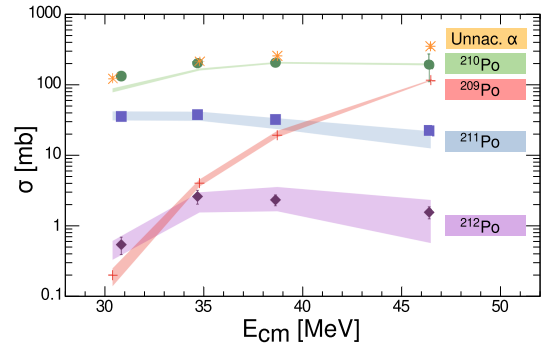


Figure 2. Deduced incomplete fusion cross sections for polonium isotopes, compared to previous direct measurements from α -decay. The coloured bands show the isotopic incomplete fusion cross sections deduced from the experimental unaccompanied α -particle cross sections (orange crosses) and their energy spectra. Previous directly measured cross-sections for ${}^{210-212}\text{Po}$ are shown by symbols as indicated. The agreement is excellent. ${}^{209}\text{Po}$ was not previously measured using α -decay spectroscopy due to the 124 year half-life. See text for further details. Adapted from Ref. [26].

Broadly, these differences suggest different reaction mechanisms for no-capture breakup and incomplete fusion.

To investigate further, it would be desirable to characterise those unaccompanied α -particles when in coincidence with heavy incomplete fusion products. This would confirm the relationship between the unaccompanied alphas and incomplete fusion, and show how these events map onto the energy-angle correlation plot (such as shown in Fig. 1). This was achieved by virtue of the short-lived α -decay of ${}^{212}\text{Po}$. ${}^{212}\text{Po}$ is produced in the transfer of a triton to the target nucleus. If no neutrons are evaporated, ${}^{212}\text{Po}$ will end up in the ground state, which undergoes α -decay, with 100% probability and a half life of 294 ns. This short lifetime allows clean measurement of coincidences with the breakup α -particle. The neutron separation energy of ${}^{212}\text{Po}$ is $S_n = 6.01$ MeV. Requiring the final product of incomplete fusion to be ${}^{212}\text{Po}$ selects transfer reactions where ${}^{212}\text{Po}$ was populated at relatively low excitation energy such that no neutron was evaporated.

The *projectile-like* α -particles in coincidence with ${}^{212}\text{Po}$ decay α -particles are shown by black and grey points in both Figure 1(a) and (b). The vast majority (black points) are concentrated at very high energies and very forward angles — exactly what one would expect for triton transfer to low excitation energy in ${}^{212}\text{Po}$. The remaining grey points are consistent with random coincidences. The black points are outside the distribution of NCBU events as seen in Figure 1(a), but lie within the distribution of unaccompanied α -particles (Figure 1(b)). There are relatively few events here in the unaccompanied α spectrum because (as can be seen) this Q-value is far from optimal — but they are consistent [26] with the tail of the distribution in Q. These results were also compared to classical dynamical model simulations [17, 21]. These reproduced the results for no-capture breakup very well, but were fun-

damentally inconsistent with the measurements of the unaccompanied α -particles.

The fact that the NCBU distribution of events does not extend so high in energy is to be expected. If breakup occurs near the barrier radius R_B , one would expect the escaping fragments to emerge with an energy approximately equal to the fragment-target Coulomb energy at that point. A mechanism whereby breakup results in such a large concentration of kinetic energy in one of the two fragments is hard to imagine. Even if incomplete fusion (and the unaccompanied α -particles) arose from events where one fragment was captured after breakup, such a mechanism requires the two fragments to be propagating independently *prior* to reaching the fusion barrier, and again it is hard to see how this could lead to such concentration of kinetic energy in the escaping fragment.

Taking the hypothesis that all the unaccompanied α -particles result from triton transfer to form ^{212}Po allows the prediction of the yields and identities of all the “incomplete fusion” products. The distribution of initial excitation energies of the ^{212}Po following the transfer can be obtained from the measured energy spectrum of the unaccompanied α particles. The excited ^{212}Po products will mostly evaporate neutrons, leading to lighter polonium isotopes ($^{209-211}\text{Po}$). Feeding the experimentally deduced excitation energy distribution for ^{212}Po into the PACE4 evaporation model, we can then estimate the isotopic incomplete fusion cross sections and compare with earlier measurements identifying them by their ground-state α -decay [3, 4]. The results are shown in Figure 2. There is excellent agreement between the present measurements and the previous direct isotopic cross sections measurements. We were also able to provide an estimate for the ^{209}Po cross section which was previously unmeasured due to the 124 year α -decay half-life.

Together, these results strongly suggest that the dominant mechanism leading to incomplete fusion and the suppression of complete fusion is direct capture of the cluster constituents by the target, without the need to produce an unbound intermediate state. The picture of incomplete fusion that emerges is essentially a geometrical one. The clustering in the projectile ground state displaces the two clusters away from its center of mass. When the projectile reaches the barrier radius R_B , one cluster is likely to have $r_1 < R_B$ and second $r_2 > R_B$. The strong nuclear interaction of the closer cluster with the target is what leads to its capture. The weaker interaction of the distant cluster mean that it is less likely to be captured, resulting in suppression of complete fusion. In the case of ^7Li , the lower Coulomb repulsion of the triton with respect to the target may allow it to get closer, hence triton-incomplete fusion is apparently much stronger than α -incomplete fusion at low energies, and the difference between the two decreases as the collision energy increases. The differing interactions of the α and triton with the target may also play a role (i.e. the distance to the target required for their capture may differ). These conclusions are consistent with recent theoretical work by Lei and Moro implementing inclusive breakup models [27–29].

4 Conclusions

Breakup is naturally present in reactions of weakly bound nuclides, and it was long thought to be responsible for the reduction in complete fusion cross-sections compared to calculations or to reactions of more strongly bound nuclides [4].

Our recent experimental work, and also recent theoretical work, lead to the conclusion that the mechanism leading to incomplete fusion is predominantly a direct, single-step process, whereby a cluster is captured by the target nucleus from the projectile ground state. This is favoured in cases where the projectile ground state is strongly clustered and those clusters are weakly bound to each other. Naturally, this circumstance also favours elastic breakup of the projectile and, in many cases, breakup mediated by the transfer of nucleons. It now seems clear that these separate phenomena are both correlated with clustering and weak-binding, but breakup is not a major cause of incomplete fusion.

Though challenging to measure, unaccompanied light fragments are a promising way to measure incomplete fusion and interrogate its mechanisms for many different projectiles and targets. One open question is whether breakup followed by capture plays any role in giving incomplete fusion. Measurements of unaccompanied tritons from $^7\text{Li}+^{209}\text{Bi}$ would be valuable: if breakup followed by capture does contribute somewhat, it may be more obvious in this case where the incomplete fusion cross sections are smaller. Measurements closer to the barrier energy may also therefore be fruitful — at some point, one might expect to see some evidence in the unaccompanied particle angular distributions. Unaccompanied clusters from ^6Li would also be very valuable.

In principle, one could attempt to measure unaccompanied particles that are not the lowest energy configuration — for example, protons or deuterons from ^7Li . This again could provide insights into the role of transfer prior to incomplete fusion, but may also require measurement of neutrons to comprehensively pin down the mechanism. It would also be very interesting to attempt to directly measure the mechanism for incomplete fusion in nuclides with three charged clusters (e.g., ^{12}C).

Whether the suppression of complete fusion persists for unstable nuclides is still unclear. Charge clustering is clearly key, and one might expect complete fusion suppression to be stronger if those charged clusters are weakly bound to each other. Our unaccompanied α -particle measurements for ^8Li [24] are consistent with the observation of fusion suppression for ^8Li [9], and $^{10,11}\text{Be}$ [2, 11, 12] also show a significant suppression. However, in all cases, the degree of suppression appears to be inconsistent with the trend observed for stable nuclides [12]. Further work is required, and more measurements of fusion, incomplete fusion and breakup would be very beneficial.

Though likely a minor contributor to incomplete fusion, the dynamics of near-barrier transfer-induced breakup are rich and complex. Our work has demonstrated the value in comprehensive measurements of breakup outcomes to probing the detail of near-barrier reaction mecha-

nisms and their timescales. Extending these measurements to exotic nuclear systems will be of great interest.

5 Acknowledgments

The authors acknowledge the Australian Research Council for their support for this body of work through Australian Research Council Grants No. FL110100098, FT120160760, DP130101569, DE140100784, DP160101254, DP170102423, DP170102318, DP190101442, DP190100256 and DP200100601. Financial support for accelerator operations was provided by the Australian National Collaborative Research Infrastructure Strategy (NCRIS) through the Heavy Ion Accelerators (HIA) project.

References

- [1] M. Dasgupta, D.J. Hinde, R.D. Butt, R.M. Anjos, A.C. Berriman, N. Carlin, P.R.S. Gomes, C.R. Morton, J.O. Newton, A. Szanto de Toledo et al., *Physical Review Letters* **82**, 1395 (1999)
- [2] A. Yoshida, C. Signorini, T. Fukuda, Y. Watanabe, N. Aoi, M. Hirai, M. Ishihara, H. Kobinata, Y. Mizoi, L. Mueller et al., *Physics Letters B* **389**, 457 (1996)
- [3] M. Dasgupta, D.J. Hinde, K. Hagino, S.B. Moraes, P.R.S. Gomes, R.M. Anjos, R.D. Butt, A.C. Berriman, N. Carlin, C.R. Morton et al., *Physical Review C* **66**, 041602 (2002)
- [4] M. Dasgupta, P.R.S. Gomes, D.J. Hinde, S.B. Moraes, R.M. Anjos, A.C. Berriman, R.D. Butt, N. Carlin, J. Lubian, C.R. Morton et al., *Physical Review C* **70**, 024606 (2004)
- [5] H. Freiesleben, H.C. Britt, J. Birkelund, J.R. Huizenga, *Physical Review C* **10**, 245 (1974)
- [6] Y.W. Wu, Z.H. Liu, C.J. Lin, H.Q. Zhang, M. Ruan, F. Yang, Z.C. Li, M. Trotta, K. Hagino, *Physical Review C* **68**, 044605 (2003)
- [7] P.R.S. Gomes, I. Padron, E. Crema, O.A. Capurro, J.O.F. Niello, A. Arazi, G.V. Martí, J. Lubian, M. Trotta, A.J. Pacheco et al., *Physical Review C* **73**, 064606 (2006)
- [8] A. Mukherjee, S. Roy, M. Pradhan, M. Saha Sarkar, P. Basu, B. Dasmahapatra, T. Bhattacharya, S. Bhattacharya, S. Basu, A. Chatterjee et al., *Physics Letters B* **636**, 91 (2006)
- [9] E.F. Aguilera, E. Martinez-Quiroz, P. Rosales, J.J. Kolata, P.A. DeYoung, G.F. Peaslee, P. Mears, C. Guess, F.D. Becchetti, J.H. Lupton et al., *Physical Review C* **80**, 044605 (2009)
- [10] L.R. Gasques, D.J. Hinde, M. Dasgupta, A. Mukherjee, R.G. Thomas, *Physical Review C* **79**, 034605 (2009)
- [11] C. Signorini, A. Yoshida, Y. Watanabe, D. Pierrousakou, L. Stroe, T. Fukuda, M. Mazzocco, N. Fukuda, Y. Mizoi, M. Ishihara et al., *Nuclear Physics A* **735**, 329 (2004)
- [12] D.J. Hinde, M. Dasgupta, *Physical Review C* **81**, 064611 (2010)
- [13] N.T. Zhang, Y.D. Fang, P.R.S. Gomes, J. Lubian, M.L. Liu, X.H. Zhou, G.S. Li, J.G. Wang, S. Guo, Y.H. Qiang et al., *Physical Review C* **90**, 024621 (2014)
- [14] D.J. Hinde, M. Dasgupta, B.R. Fulton, C.R. Morton, R.J. Wooliscroft, A.C. Berriman, K. Hagino, *Physical Review Letters* **89**, 272701 (2002)
- [15] V. Tripathi, A. Navin, K. Mahata, K. Ramachandran, A. Chatterjee, S. Kailas, *Physical Review Letters* **88**, 172701 (2002)
- [16] K. Hagino, M. Dasgupta, D. Hinde, *Nuclear Physics A* **738**, 475 (2004)
- [17] A. Diaz-Torres, D.J. Hinde, J.A. Tostevin, M. Dasgupta, L.R. Gasques, *Physical Review Letters* **98**, 152701 (2007)
- [18] R. Rafiei, R.d. Rietz, D.H. Luong, D.J. Hinde, M. Dasgupta, M. Evers, A. Diaz-Torres, *Physical Review C* **81**, 024601 (2010)
- [19] D. Luong, M. Dasgupta, D. Hinde, R.d. Rietz, R. Rafiei, C. Lin, M. Evers, A. Diaz-Torres, *Physics Letters B* **695**, 105 (2011)
- [20] D.H. Luong, M. Dasgupta, D.J. Hinde, R. du Rietz, R. Rafiei, C.J. Lin, M. Evers, A. Diaz-Torres, *Physical Review C* **88**, 034609 (2013)
- [21] E.C. Simpson, K.J. Cook, D.H. Luong, S. Kalkal, I.P. Carter, M. Dasgupta, D.J. Hinde, E. Williams, *Physical Review C* **93**, 024605 (2016)
- [22] S. Kalkal, E.C. Simpson, D.H. Luong, K.J. Cook, M. Dasgupta, D.J. Hinde, I.P. Carter, D.Y. Jeung, G. Mohanto, C.S. Palshetkar et al., *Physical Review C* **93**, 044605 (2016)
- [23] K.J. Cook, E.C. Simpson, D.H. Luong, S. Kalkal, M. Dasgupta, D.J. Hinde, *Physical Review C* **93**, 064604 (2016)
- [24] K.J. Cook, I.P. Carter, E.C. Simpson, M. Dasgupta, D.J. Hinde, L.T. Bezzina, S. Kalkal, C. Sengupta, C. Simenel, B.M.A. Swinton-Bland et al., *Physical Review C* **97**, 021601 (2018)
- [25] A. Horsley, D. Hinde, M. Dasgupta, R. Rafiei, A. Wakhle, M. Evers, D. Luong, R. du Rietz, *Nuclear Instruments and Methods in Physics Research Section A: Accelerators, Spectrometers, Detectors and Associated Equipment* **646**, 174 (2011)
- [26] K.J. Cook, E.C. Simpson, L.T. Bezzina, M. Dasgupta, D.J. Hinde, K. Banerjee, A.C. Berriman, C. Sengupta, *Physical Review Letters* **122**, 102501 (2019)
- [27] J. Lei, A.M. Moro, *Physical Review C* **92**, 044616 (2015)
- [28] J. Lei, A.M. Moro, *Physical Review C* **95**, 044605 (2017)
- [29] J. Lei, A.M. Moro, *Physical Review Letters* **123**, 232501 (2019)